REPORT : Exploration of the Midnight Owl Lithium Pegmatite Project, Yavapai County, Arizona, USA

Outcrop of the Midnight Owl pegmatite. Jeep for scale. Photo by the Author.

BrightRock Gold Corp.

April 18, 2024

By:
James Ingraffia, MS, GMBA

Lithium Arrow LLC

Forward Looking Statement

BrightRock Gold Corp. understands, acknowledges, and agrees that all predictions, projections, results, technical studies and/or all other reports concerning the Midnight Owl Lithium Project, the subject matter of this report, economic performance and/or BrightRock Gold's plans and objectives for management and development of the Midnight Owl Lithium Project, constitute forward-looking statements made pursuant to the safe harbor provisions of Section 21 E of the Securities Exchange Act of 1934, as amended, and Section 27 A of the Securities Act of 1933, as amended that involve risks and uncertainties. Although it is believed that the expectation reflected in such forward-looking statements are reasonable, the forward-looking statements and financial projections contained in various documents related to BrightRock Gold Corp. and the development of the Midnight Owl Lithium Project are subject to risks and uncertainties that could cause actual results to differ from those projected. Generally, any statements that are not historical facts may contain forward looking information, and forward looking information can be identified by the use of terminology including, but not limited to, “plans”, “estimations”, “expects”, “it would take”, “could”, “would”, “might”, and “forecasts”. Technical drafts and information contained within this document is subject to change with new and future information. Investors and decision makers, including but not limited to BrightRock Gold Corp., are cautioned that any forward-looking statements and projections are not guarantees of future performance or exactness of nature and that actual results may differ materially from those in the forward-looking statements. Factors that could cause actual results to differ materially from those reflected in forward-looking statements include, but are not limited to, new information, risks and uncertainties regarding the actual precious metals mineralization of the Midnight Owl Lithium Project, fluctuations in precious metals market prices, and inflationary trends occurring with respect to costs associated with mine development and minerals extraction operations.

Table of Contents

Table of Tables

Table of Figures

Summary

The project covers 5,000 acres and underwent a four-day mapping and sampling exercise. Geological mapping revealed the presence of pegmatites within Precambrian metasediments and Tertiary volcanic rocks. Samples collected from the pegmatites showed mineralogical composition typical of lithium-bearing pegmatites, with assays indicating lithium concentrations and correlation with other elements. Analysis of K:Rb ratios suggested potential for lithium mineralization, particularly in northeast regions. Future work includes soil sampling surveys to further assess lithium potential. Overall, the report highlights promising geological characteristics and outlines a strategy for further exploration.

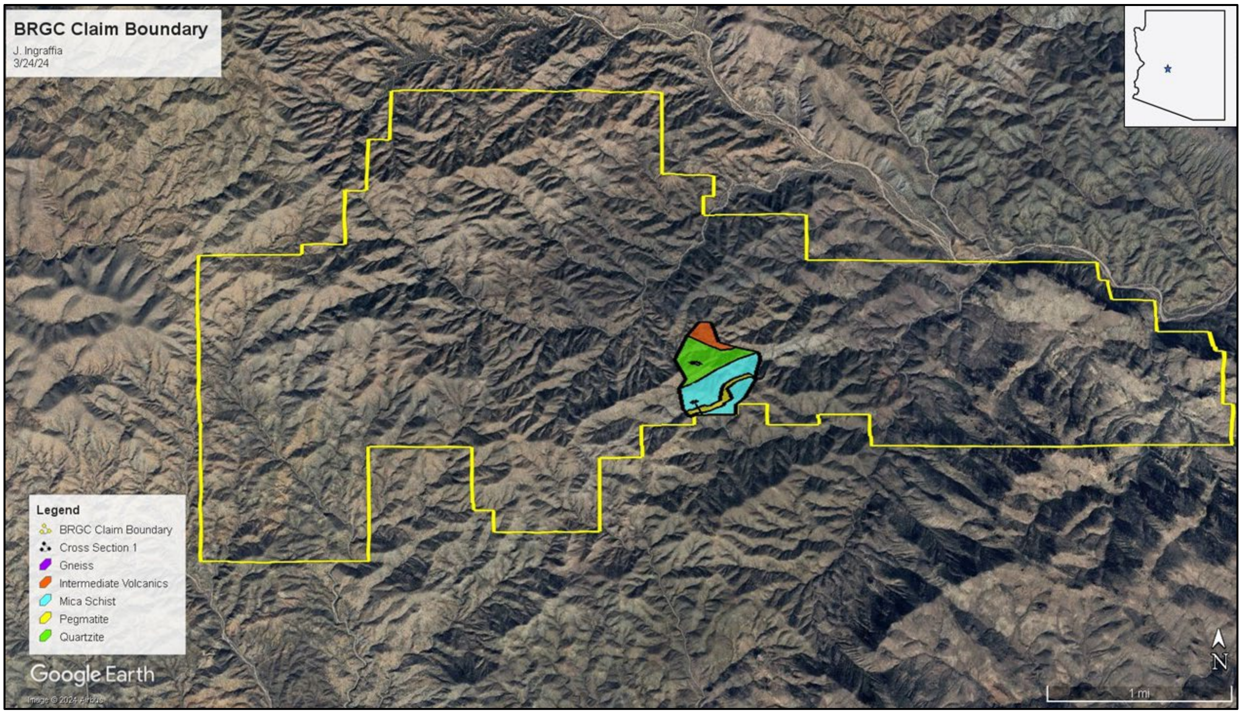

Figure 1: Brightrock Gold Corp. Claim Boundary and Mapped Area.
The BRGC claim boundary is delineated by the yellow outline, positioned at the star within the Arizona inset map. The colored area (red, green, blue) represents the geological mapping conducted in this study. Yellow pins on the map indicate sampling locations undertaken during this survey.

Location

The BRGC Midnight Owl project is situated within the White Picacho Mining District, located in Yavapai County, West-Central Arizona. Covering an expansive area of approximately 5,000 acres across 243 parcels. Positioned approximately 30 miles northwest of Phoenix and 10 miles east of the nearest town, Wickenburg, the Midnight Owl project occupies a strategically located region within the state.

Throughout 2023, the project boundary has undergone several expansions through dedicated exploration initiatives by the company. These expansions were implemented to more effectively target lithium mineralization potential within the region. The boundary adjustments aimed to encompass further historical gold workings (Mindat, 2024).

The local pegmatitic mineralization encompasses a variety of valuable elements such as lithium, beryllium, feldspar, and mica. Additionally, minor commodities including bismuth, copper, lead, silver, and zinc are present within the region. Hydrothermal-emplacement gold deposits have also been identified in the area, further enriching its mineral diversity (Meeves et al., 1966).

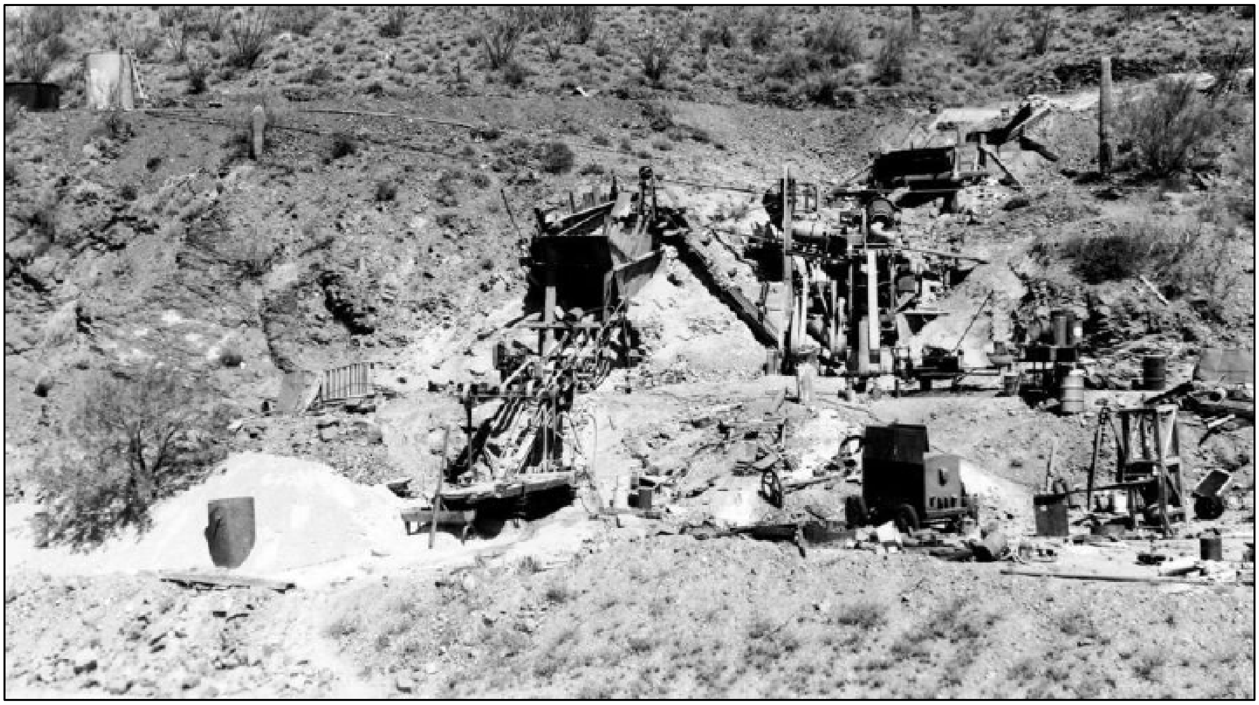

Figure 2: Historic workings of pegmatite lithium in the White Picacho district.
From (Ascarza, 2016).

The White Picacho district boasts a rich history of lithium production from spodumene, beryl, and columbite/tantalum minerals, alongside significant yields of mica. Between 1941 and 1963, small-scale mining operations yielded substantial quantities, including 62 tons of lithium ore, 154,255 lbs of beryl, 40,117 tons of scrap mica, and 5,900 lbs of columbite-tantalum minerals, as documented by Ascarza (2016). Additionally, the district has recorded commercially viable reserves of feldspar.

Project Scope

This report denotes a four-day reconnaissance mapping and sampling exercise to familiarize the company with the geology with respect to lithium pegmatite mineralization. Approximately 101 acres were mapped in the southern portion of the BRGC claim area. Sampling was conducted on an exposed pegmatite ridgeline through the southern portion of the claims. A total of 20 samples were collected to begin the assay campaign aimed at vectoring into lithium ore bodies. They were sent to ALS Global for chemical analyses in Reno, Nevada. Of those samples, 10 are from an exposed pegmatite, and are the subject matter considered here. The area selected to map was determined by satellite imagery and previous site visits.

Geology

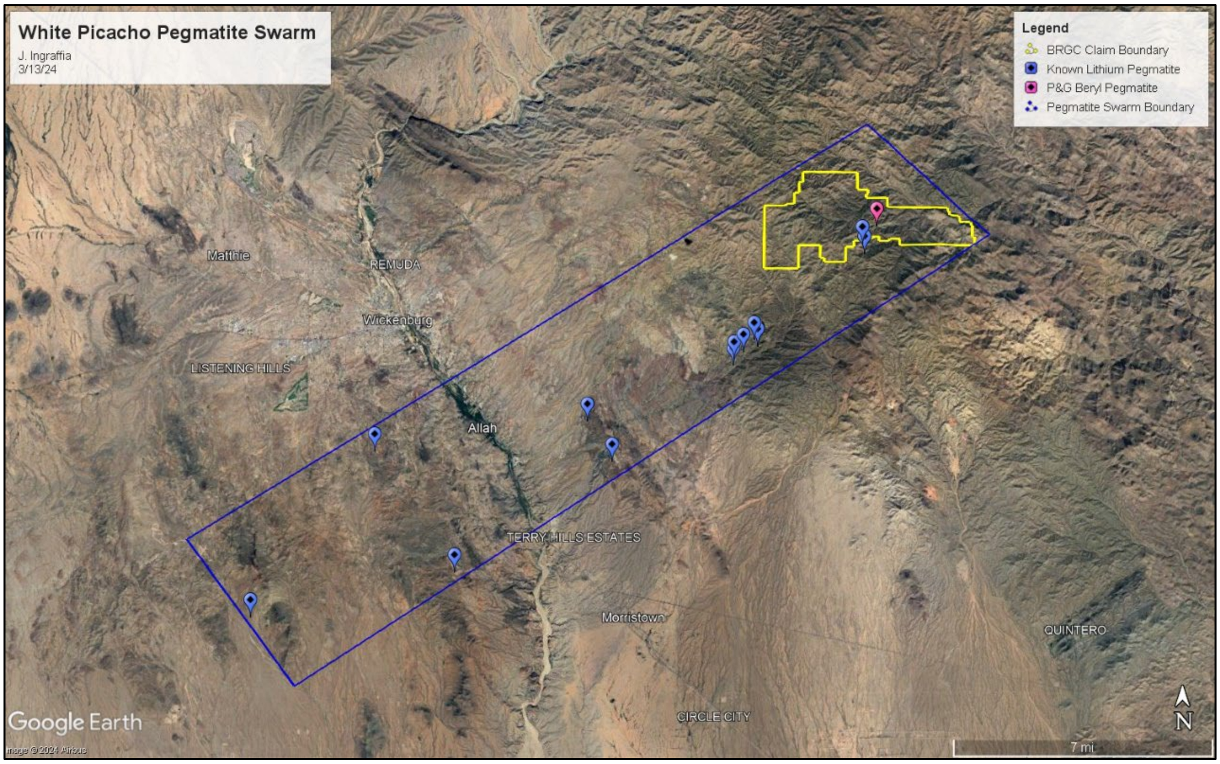

Figure 3: Pegmatite swarm map, local White Picacho District area, AZ, USA.
Note the NE trend of the pegmatite swarm. Data from London and Burt (1978), Mindat (2024); Sunderland (2023).

Geologic Setting

BRGC's Midnight Owl lithium pegmatite project is located in the Mexican Highlands mountain belt in Arizona, between the faulted Great Basin to the southwest and the Colorado Plateau to the northeast. The project similarly is centrally located in the greater Arizona pegmatite belt, that extends from the northwest corner of the state southeastward in the direction of Phoenix (London and Burt, 1982). The pegmatites in the district have been thoroughly described in comprehensive mineralization references (Guilbert and Park, 1986). The Precambrian and Tertiary rocks in the study area are reportedly to be heavily faulted and sheared; the reader is encouraged to see Jahns, (1952) for more detailed information.

The claim parcels are located on the north side of a significant pegmatite swarm (Figure 1, Table 1). A minimum of 14 Li bearing pegmatites trend from SW to NE, not including a historic beryl pegmatite on the BRGC property. Pegmatite that matches descriptions of potentially lithium-bearing ore rock are located within the claim boundary.

Reconnassiance level, local geology is primarily divided into Precambrian metasediments referred to here as the Yavapai formation, Precambrian pegmatite, and Tertiary volcanics. Cretaceous granites and Tertiary conglomerates have also been described previously in the area. The Yavapai formation rocks are capped by the Tertiary volcanic rocks and conglomerates. Intermediate-composition volcanic rocks uncomformably contact the Yavapai formation at an erosional boundary. BRGC has identified what appears to be "pegmatite stockwork" within the intermediate volcanic rocks in a wash through the project area; the company speculates that the stockwork is remobilized lithium at depth by post-magmatic metasomatism.

Number	Pegmatite Name	Li Mineral
1	Midnight Owl Open Cut	Spodumene, Lepidolite
2	Independence Mine	Spodumene, Lepidolite, Montebrasite, Eucryptite, Lithiophilite
3	Lone Giant*	Spodumene, Lepidolite, Montebrasite, Lithiophilite
4	White Ridge*	Spodumene, Montebrasite, Lithiophilite
5	Picacho View	Spodumene, Lepidolite, Montebrasite
6	White Jumbo	Spodumene, Lepidolite, Montebrasite
7	Sunrise Prospect	Spodumene, Lepidolite, Montebrasite
8	Lower Jumbo	Spodumene
9	Morning Star	Spodumene, Lepidolite, Montebrasite, Lithophilite, Amblygonite
10	Dragon Mine	Lepidolite
11	San Domingo	Spodumene(?)
12	Ambly Mine	Lepidolite
13	Unnamed Li Occurrence	Lepidolite
14	Boyd Forner Prospect	Lepidolite

Table 1: Li-bearing pegmatites in the White Picacho District and into the proximal southwest areas, Arizona. From Jahns (1952); Mindat (2024); and Sunderland (2023).

White Picacho district pegmatites are found as off-white, resistant, irregular dikes and lenses. They can be hosted within Precambrian metasedimentary rocks, specifically the Yavapai formation quartz mica schists and geneisses, or a nearby granitic pluton of the same age. The pegmatite on company ground is hosted within the Yavapai formation quartz-mica schist. The pegmatites are reportedly Precambrian aged, and locally trend NE – SW with the strike of the host Yavapai metasedimentary rocks.

Geologic Mapping Phase 1

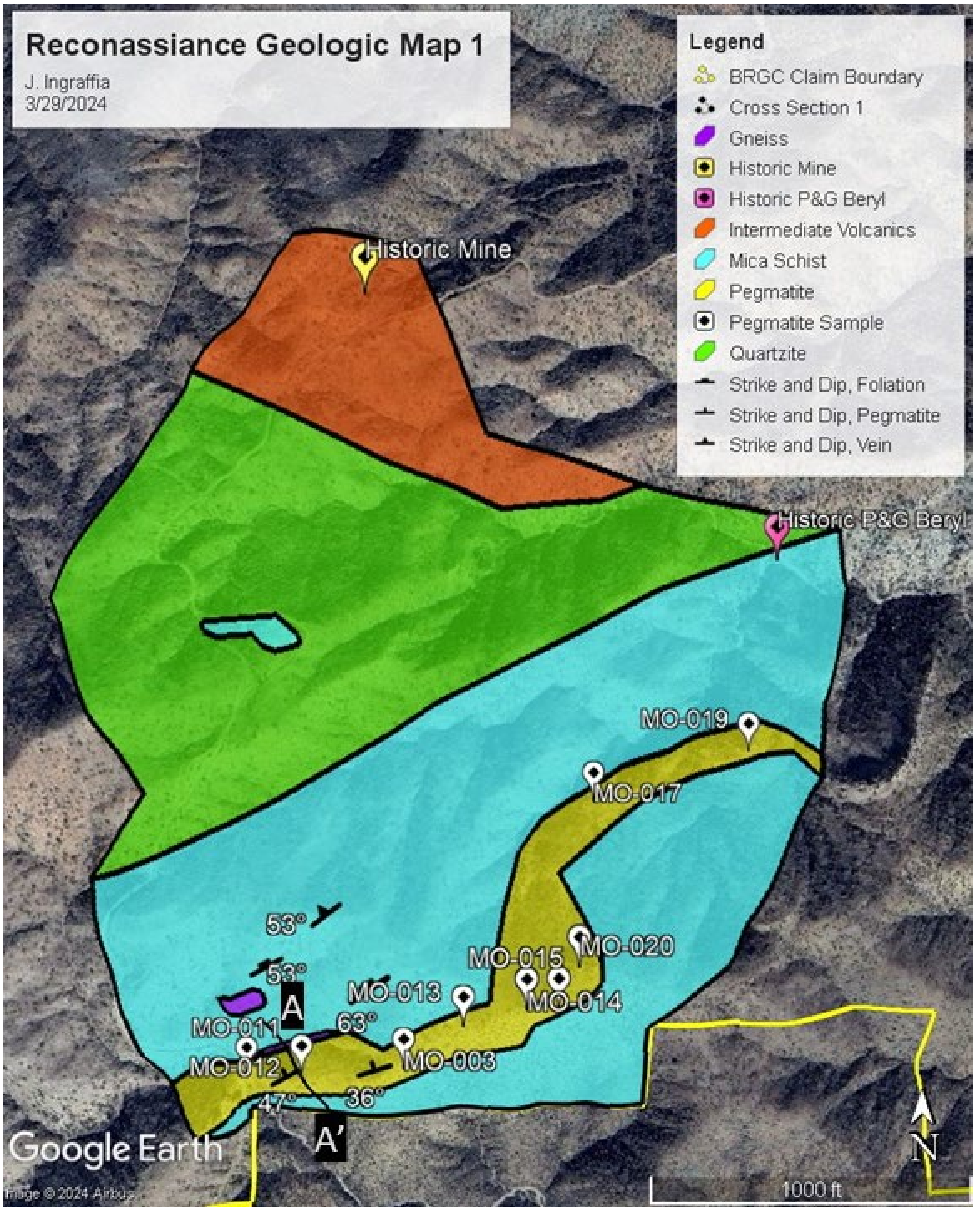

Figure 4: Reconnassiance geologic map of the Midnight Owl project area.

The geologic map was meticulously crafted over a span of four days of fieldwork. On the 1st and 4th days, field reconnaissance commenced from the southern entrance, focusing on detailed examinations of the pegmatite and its associated host mica schist formations (Figures 1, 4 and 5). The 2nd day was dedicated to surveying outlier regions along the northern claim boundary. On the 3rd day, the study area was observed from a northern perspective, traversing through the intermediate volcanic formations and proceeding southward into the quartzite terrain.

Footnote: Company records indicate that the Historic Mine in the volcanic formation was for gold and copper; However, study of that mine is out of scope of this report (Figure 4, 5; Brightrock Gold Corp, 2017).

Unit Descriptions

The geology of the Midnight Owl project area presents a compositionally complex landscape, characterized by the juxtaposition of unconformable rock types originating from vastly different ages and origins. Ground truthing efforts have revealed Tertiary rocks situated to the north juxtaposed against Precambrian formations to the south. The rugged terrain is marked by numerous ravines that traverse the landscape. Fieldwork has corroborated the geological descriptions outlined in prior studies, such as those by London and Burt (1978).

The Tertiary-aged dacitic intermediate volcanic rocks (red in Fig. 4, 5) serve as the host for a historic gold mine situated in the northern sector of the study area. An adit, positioned at the base of the hill to the northeast, provides access to these workings within the dacitic rock formation. Notably, these workings are in close proximity to the sharp contact with the adjacent Precambrian quartzite, highlighting the geological significance of their location.

The Precambrian impure quartzites (green) constitute the subsequent rock formation encountered during a north-south traverse through the study area. Characterized by its lateral expansiveness, the quartzite demonstrates a predominant NE-SW trend. Within this quartzite formation, sporadic occurrences of quartz veins containing accessory muscovite books, measuring up to 1 cm^3 in volume*. Moving southward, localized outcrops of quartz mica schist are observed within the quartzite matrix.

In this study, the interpretation of the contact between the Precambrian impure quartzite and quartz mica schist (blue in Fig. 4, 5) was conducted with adherence to best practices. This interpretation was informed by a comprehensive approach, integrating landform evaluation, analysis of surrounding geological data, satellite imagery, and comparison with available hyperspectral geophysics data (Brightrock Gold Corp., 2023). Figures 1, 4, and 5 provide visual representations of the quartzite-schits contact interpretation. It is important to note that the examination of lands to the south was conducted by entry from the south, as opposed to the previously stated approach of traversal from the north.

The schist itself exhibits pronounced foliation, presenting a silvery coloration characteristic of metasedimentary rock prone to rapid erosion. These visual characteristics align with observations made by Jahns (1952) and London and Burt (1978), where both eroded and fresh surfaces display a blue-silver hue, contrasting with weathered surfaces that adopt a gold-brown appearance. The presence of large divots along the road through the schist underscores the rapidity of its weathering processes. Additionally, occasional lenses of gneiss are locally embedded within the schist, as illustrated in Figures 4 and 5. The dip-dip direction of foliation varies between 63º/326º azimuth and 53º/322º degrees azimuth. Furthermore, quartz stringers traversing the schist maintain a consistent concordance, aligning at 53º/322º azimuth (northernmost measurement, Figures 4, 5).

*See it on YouTube: https://www.youtube.com/watch?v=XSwKLl7pqfA

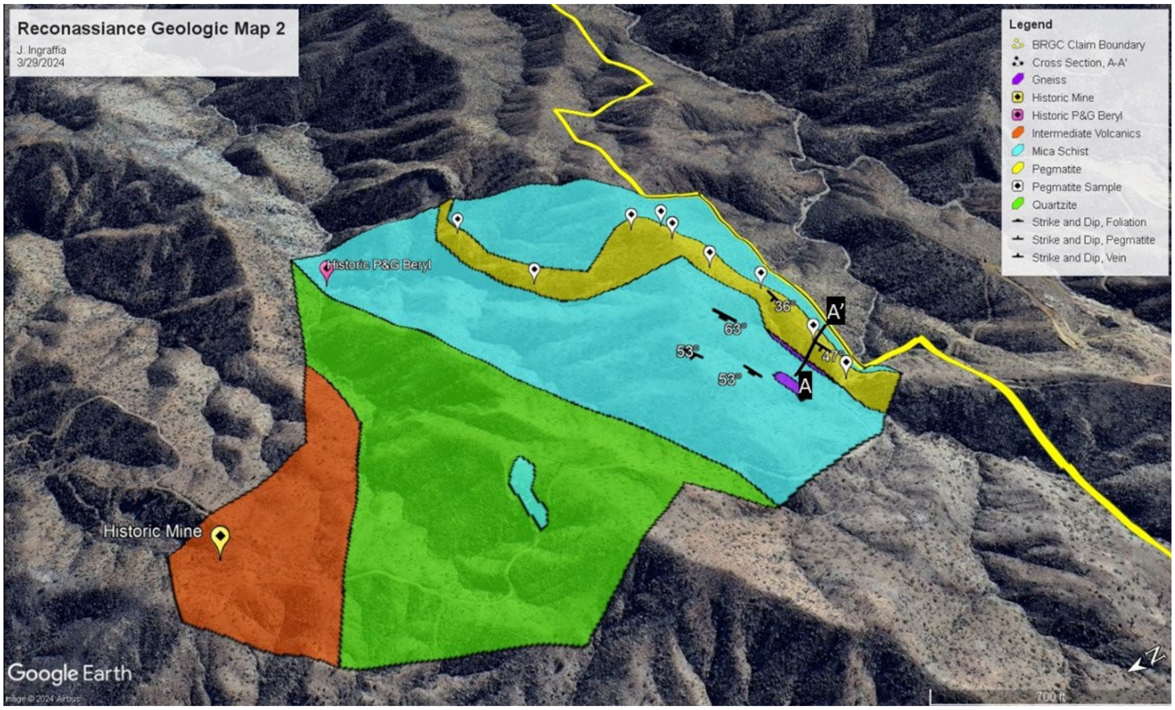

Figure 5: Alternate view of the geologic map.
Note the topographic relief of the study area.

The mapped volume of pegmatite, colored yellow in Figures 4 and 5, extends approximately 0.5 mi NE-SW. At cross-section line A-A', the pegmatite measures approximately 200 ft in thickness, with a dip-dip direction recorded at 47º/332º azimuth (Figures 5 and 6). This intrusive feature traverses the schist, displaying a moderate concordance to moderate discordance with the foliation dip, yet aligns closely with the strike of the foliation. This observation corroborates findings from previous studies, such as those outlined by London and Burt (1978), which detail generalized behaviors of local pegmatites. Notably, fractures along the ridgeline of the pegmatite exhibit concordance along the pegmatite strike. Despite the predominantly linear nature of the pegmatite dike, it deviates northwestward briefly before resuming its northeastward trajectory.

The northwestward deviation in the trend of the pegmatite is notably observed in Section 50, coinciding with the presence of a small historical sample pit and distinct contacts with the surrounding host mica schist. Nearby, scattered historical markers were identified, further highlighting the significance of this location. Samples MO-014, -015, and -016 were collected from this site, as detailed in Tables 2, 3, and depicted in Figures 7 and 8.

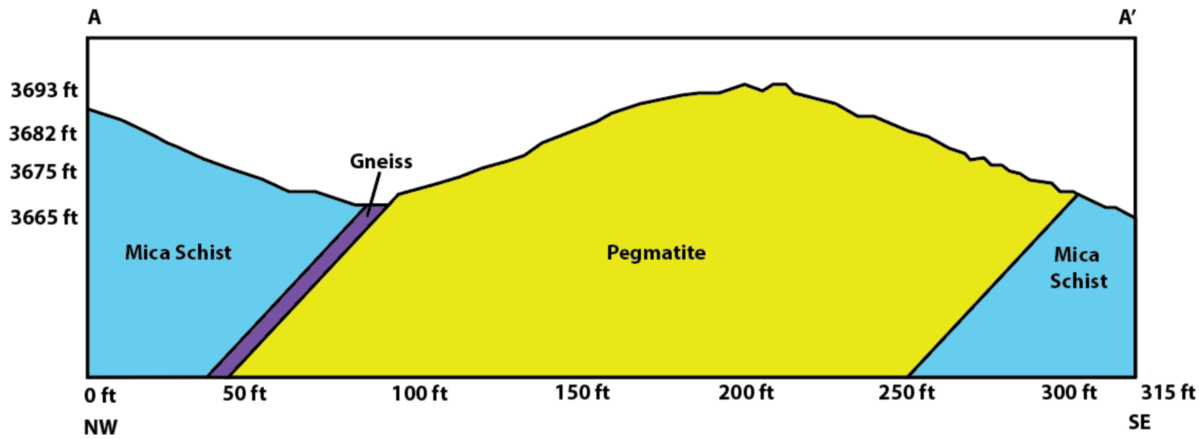

Figure 6: Cross Section A-A'.
The pegmatite, in yellow, measures approximately 200 ft in thickness and tilts about 45º NW. It is bordered by both the mica schist and gneiss to the northwest and by mica schist to the southeast.

Sampling

This report is dedicated to the analysis of pegmatite samples within the mapped area. A total of ten pegmatite samples were collected from claims 243, 46, and 50, as detailed in Table 2 and illustrated in Figures 7 and 8. These pegmatite samples underwent comprehensive analyses, including mineralogical examinations (see Figure 9), assays (refer to Table 3), determination of correlative elements to lithium, and assessment of K:Rb ratios (depicted in Figure 10). While additional samples were taken from the background country rock, their analysis falls outside the scope of this report.

Sample #	Claim
MO-003	#243
MO-011	#243
MO-012	#243
MO-013	#243
MO-014	#243
MO-015	#243
MO-016	#243
MO-017	#46
MO-019	#50
MO-020	#243

Table 2: Pegmatite sample numbers and associated claim.

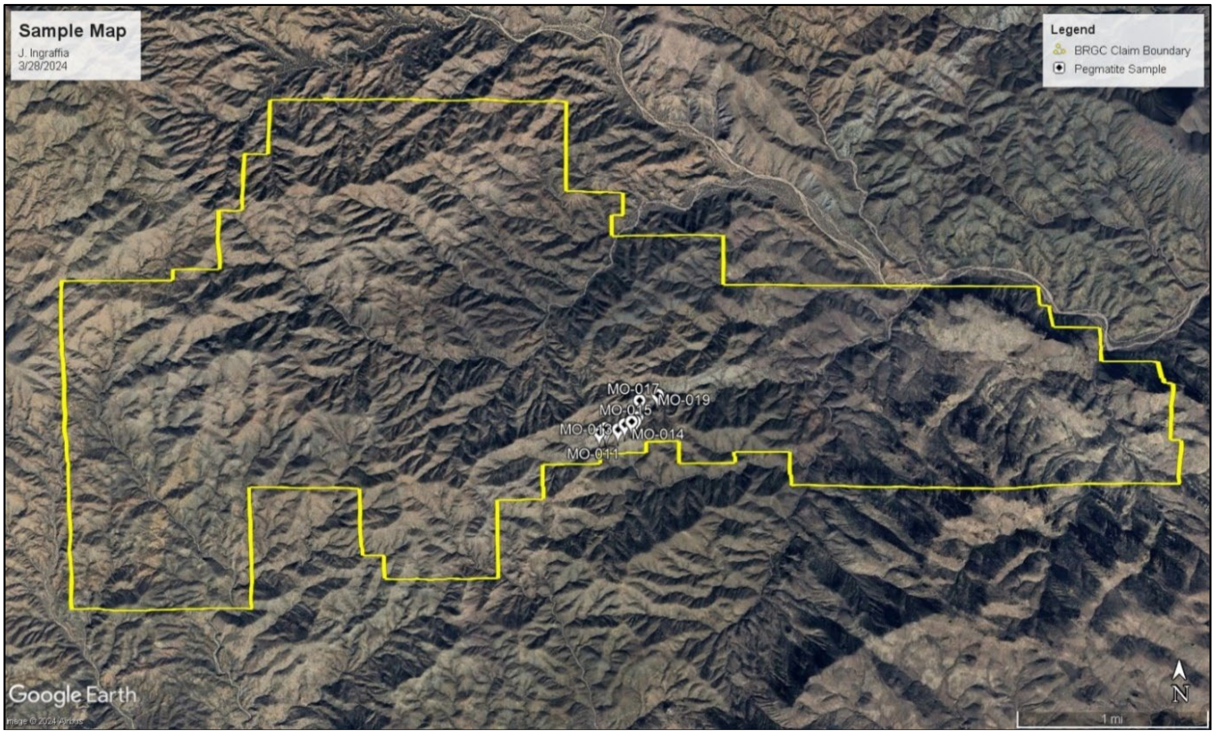

Figure 7: BRGC claim boundary and pegmatite sample locations.
Samples were taken from three areas decided by potential for mineralization.

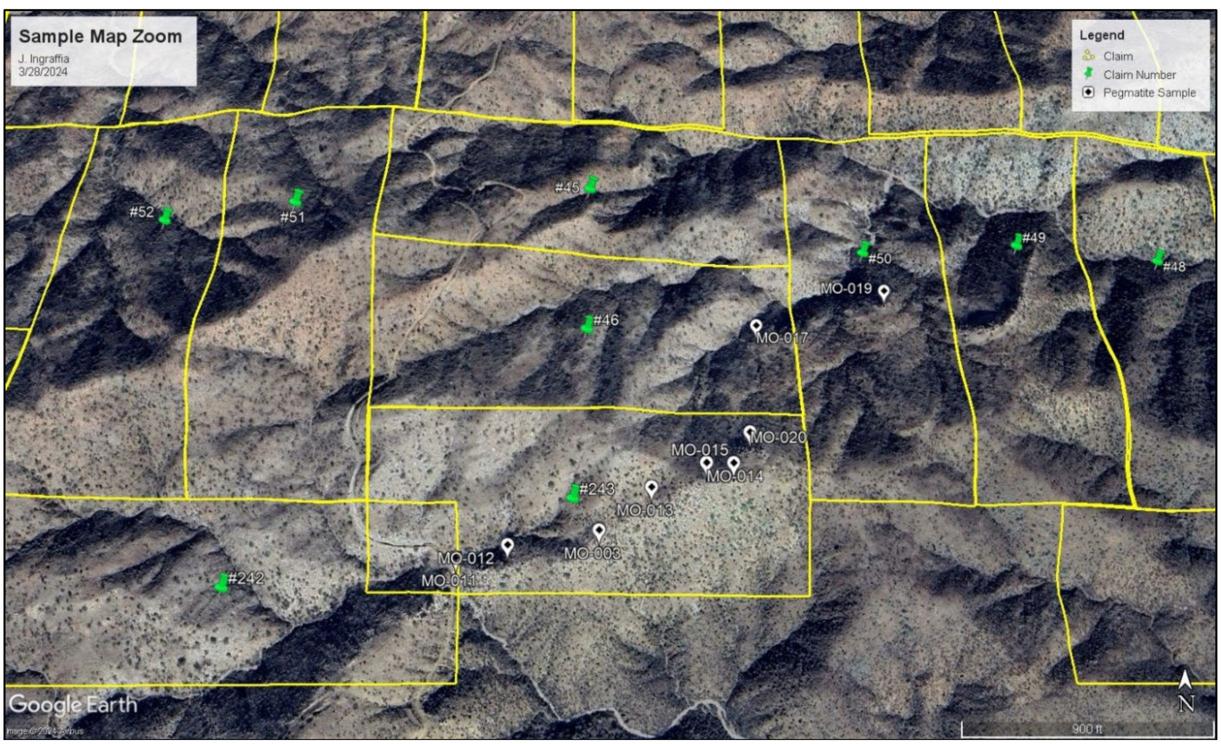

Figure 8: Samples MO-003, -011 to -017, and -019 to -020.
Taken from sections 243, 46, and 50. This area has exposed surface pegmatite (see cover photo).

Pegmatite Description

Several samples of the pegmatite trend (samples -014, -015, -016, -019) were meticulously analyzed to assess variations in modal mineralogy along the strike. Sample MO-015, showcased in Figure 9, serves as a representative average pegmatite specimen. The mineralogical composition predominantly comprises quartz and feldspar matrix, accompanied by accessory muscovite and occasional schorl. Notably, the abundance of schorl exhibits variability across the samples.

Figure 9: Sample MO-015. Sample pegmatite from historical workings.
Constituent mineralogy includes quartz, albite, accessory muscovite, and rare black tourmaline. Sample MO-015 is representative of the average mineralogy in the gathered pegmatite samples.

Figure 10: Sample MO-019.
Blocky, salmon orthoclase mineralogy is representative of pegmatite intermediate zone. Muscovite is visible on the left side of the sample. Pen for scale.

A significant alteration in modal mineralogy was observed at sample location MO-019. There salmon-colored orthoclase feldspar was identified, supplementing the existing albite and quartz matrix composition (refer to Figures 10 and 11). Notably, this location, situated approximately 50 ft above the historical P&G beryl mine in claim number 50, signifies a notable mineralogical variation within the pegmatite formation. It is noteworthy that the mineralogical descriptions of the pegmatite samples closely align with historical observations documented by Jahns (1952) and London and Burt (1978).

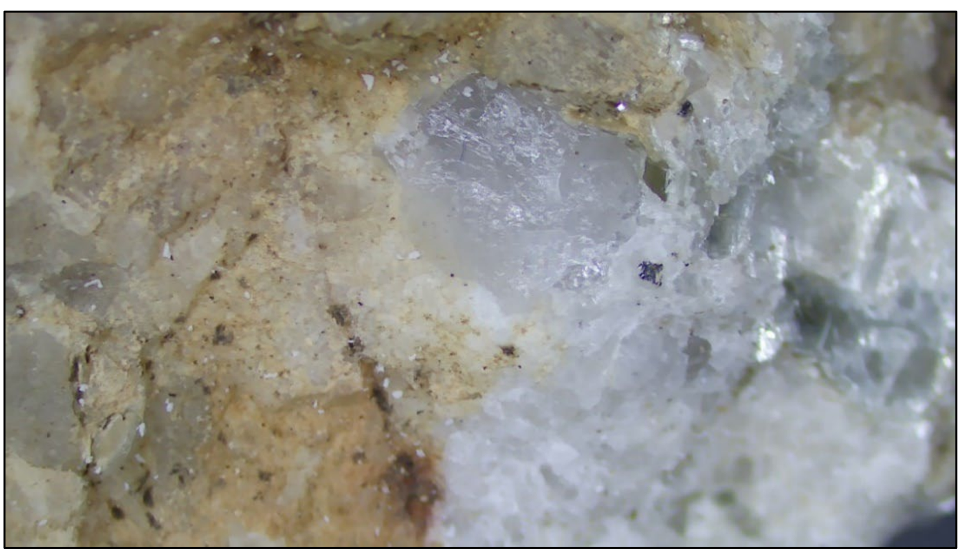

Figure 11: Zoom of sample MO-019.
Sample was inspected under microscope in Nevada Bureau of Mines and Geology. The orthoclase (salmon) mantles quartz (translucent grey) from the left of view to center, that transitions to muscovite (reflective grey) on the right. Small accessory schorl grains (black).

Assays

The assays conducted on the pegmatite samples revealed lithium concentrations ranging from 0.6 to 2.8 ppm Li. Notably, samples MO-003 and -014 exhibited the highest lithium concentrations, registering at 1.9 ppm Li and 2.0 ppm Li respectively (refer to Table 3). Additionally, tantalum (Ta) values ranged from non-detectable (represented as negative) to 0.025 ppm Ta in sample MO-014. Further analysis utilizing a Spearman correlation matrix identified several elements correlating with lithium, including Al, Be, Ce, Cr, Fe, Ga, Mg, Ni, and Zn. The elements Al, Cr, Fe, Ga, Mg, Ni, and Zn demonstrated correlation coefficients exceeding 0.6, indicating a strong correlation with lithium. Geochemistry of Be and Ce exhibited correlation coefficients near 0.4, indicating moderate correlation with lithium. Conversely, Na, Nb, and Ta displayed moderate anticorrelation with lithium in these samples, with correlation coefficients ranging from -0.3 to -0.4.

SAMPLE	DESCRIPTION	MO-003	MO-011	MO-012	MO-013	MO-014	MO-015	MO-016	MO-017	MO-019	MO-020
Recvd Wt.	kg	0.83	0.79	0.57	0.38	0.7	0.59	0.63	0.7	0.78	0.63
Au	ppm	0.0003	0.0002	0.0003	-2E-04	0.0002	-2E-04	0.0002	-2E-04	0.0003	0.0003
Ag	ppm	0.073	0.119	0.109	0.08	0.065	0.117	0.066	0.051	0.169	0.057
Al	%	0.2	0.21	0.25	0.18	0.25	0.18	0.2	0.24	0.18	0.3
As	ppm	1.28	1.92	0.89	0.95	0.5	0.79	1.1	0.71	1.5	0.81
B	ppm	-10	-10	-10	-10	30	-10	-10	-10	-10	-10
Ba	ppm	14.2	13.8	5.4	10.5	7.6	7.8	9.4	9.2	10	22.8
Be	ppm	0.29	0.37	0.34	0.2	0.37	0.22	0.24	0.31	0.4	0.5
Bi	ppm	1.03	1.305	2.72	1.36	0.812	1.295	0.985	1.715	1.355	0.462
Ca	%	0.15	0.28	0.1	0.08	0.07	0.07	0.08	0.12	0.13	0.27
Cd	ppm	0.067	0.087	0.036	0.046	0.032	0.045	0.036	0.057	0.056	0.123
Ce	ppm	1.425	2.94	1.725	1.4	29.9	1.05	1.17	1.39	3.16	2.14
Co	ppm	0.894	0.344	0.302	0.23	0.207	0.267	0.212	0.327	0.921	0.323
Cr	ppm	4.23	3.39	7.26	2.76	7.16	4.71	5.46	6.86	3.32	3.37
Cs	ppm	0.844	0.616	1.315	1.095	1.785	0.654	0.641	1.725	0.842	1.89
Cu	ppm	9.19	9.13	5.28	3.09	3.08	4.63	2.19	2.41	5.11	4.26
Fe	%	0.245	0.204	0.33	0.238	0.191	0.235	0.246	0.19	0.216	0.198
Ga	ppm	0.621	0.738	1.285	0.642	1.4	0.774	0.832	1.04	0.682	1.265
Ge	ppm	0.016	0.018	0.017	0.018	0.043	0.012	0.013	0.015	0.02	0.021
Hf	ppm	0.027	0.021	0.01	0.007	0.013	0.007	0.008	0.01	0.009	0.013
Hg	ppm	0.08	0.006	-0.004	-0.004	-0.004	0.005	0.011	-0.004	-0.004	0.013
In	ppm	-0.005	-0.005	-0.005	-0.005	-0.005	-0.005	-0.005	-0.005	-0.005	-0.005
K	%	0.07	0.08	0.12	0.12	0.14	0.09	0.11	0.13	0.06	0.12
La	ppm	0.652	1.095	0.739	0.559	12.8	0.495	0.525	0.663	1.445	0.983
Li	ppm	1.9	0.8	1	0.6	2	0.9	0.6	0.8	1.4	1.3
Mg	%	0.02	0.01	0.01	0.01	0.01	0.01	0.01	0.01	0.01	0.01
Mn	ppm	47.4	91.7	58.4	49.5	47.3	47.5	35.3	72.8	52.8	166.5
Mo	ppm	0.56	0.45	0.89	0.42	0.88	0.61	0.71	0.96	0.48	0.44
Na	%	0.077	0.088	0.062	0.049	0.035	0.057	0.067	0.051	0.081	0.091
Nb	ppm	0.742	0.638	0.559	0.308	0.819	0.647	0.952	0.469	0.282	0.62
Ni	ppm	0.78	0.69	0.84	0.44	0.54	0.61	0.53	0.77	0.55	0.6
P	%	0.054	0.114	0.037	0.027	0.029	0.025	0.026	0.045	0.054	0.107
Pb	ppm	6.67	3.97	2.72	5.64	3.39	4.5	3.35	2.36	8.39	7.22
Pd	ppm	-0.001	0.002	0.001	-0.001	-0.001	-0.001	-0.001	-0.001	-0.001	-0.001
Pt	ppm	-0.002	-0.002	-0.002	-0.002	-0.002	-0.002	-0.002	-0.002	-0.002	-0.002
Rb	ppm	8.2	8.41	17.85	16.9	22.5	14.3	14.25	20.8	10.15	19.2
Re	ppm	-2E-04	-2E-04	-2E-04	-2E-04	-2E-04	-2E-04	-2E-04	-2E-04	-2E-04	-2E-04
S	%	0.01	-0.01	0.01	-0.01	-0.01	-0.01	-0.01	-0.01	-0.01	-0.01
Sb	ppm	0.123	0.466	0.065	0.079	0.067	0.043	0.062	0.056	0.089	0.11
Sc	ppm	0.178	0.162	0.225	0.157	0.307	0.137	0.138	0.174	0.137	0.209
Se	ppm	0.028	0.014	0.005	0.004	0.011	0.006	0.007	0.006	0.014	0.016
Sn	ppm	0.07	0.08	0.4	0.13	0.54	0.25	0.27	0.33	0.14	0.37
Sr	ppm	4.93	4.52	3.23	2.66	2.6	2.16	2.56	2.6	5.35	5.3
Ta	ppm	0.008	0.005	0.011	-0.005	0.025	0.005	0.016	-0.005	-0.005	-0.005
Te	ppm	0.059	0.095	0.067	0.035	0.007	0.056	0.027	0.021	0.021	0.005
Th	ppm	1.4	1.01	1.05	0.549	11.3	0.537	0.872	0.323	1.695	0.471
Ti	%	0.001	0.001	0.001	0.001	0.002	0.001	0.001	0.001	-0.001	0.001
Tl	ppm	0.032	0.033	0.066	0.071	0.081	0.052	0.055	0.082	0.04	0.074
U	ppm	1.105	0.89	0.481	0.521	1.17	0.491	0.879	0.313	0.303	0.294
V	ppm	0.8	0.8	1	0.6	0.9	0.5	0.6	0.5	0.5	0.7
W	ppm	0.217	0.383	0.245	0.121	0.254	0.163	0.207	0.141	0.12	0.254
Y	ppm	2.27	4.03	1.59	1.145	4.17	1.165	1.615	1.12	1.17	2.85
Zn	ppm	3.5	4.1	2.3	1.9	3.4	1.9	1.2	1.7	3	3
Zr	ppm	0.69	0.48	0.26	0.19	0.44	0.23	0.25	0.3	0.14	0.45

Table 3, previous: Assays of pegmatite samples.
Lithium is highlighted in blue. Potassium and rubidium are highlighted in orange. Correlative elements are shaded in grey.

K:Rb Ratios

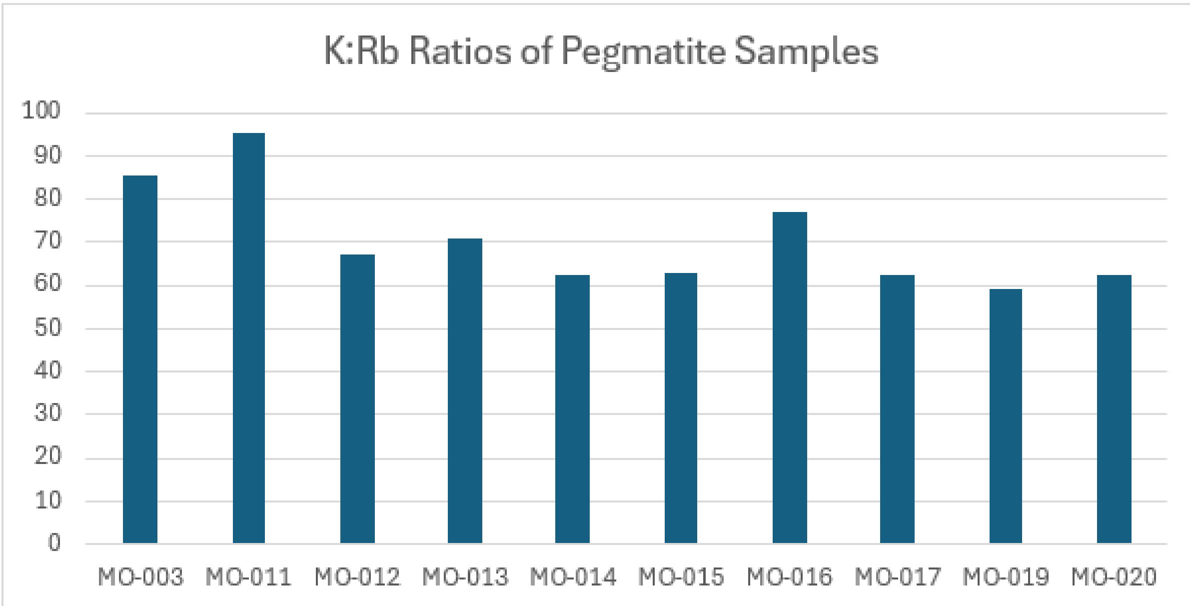

Figure 12: K:Rb ratios of Midnight Owl pegmatite samples from Table 2.
Sample locations are in Table 1, and Figures 7a and 7b. Lower ratios indicate a higher potential to indicate nearby lithium mineralization (Steiner, 2019).

Measurements of K:Rb ratios were conducted on the pegmatite samples (refer to Figure 12 and Table 4). The average K:Rb ratio across all samples was calculated to be 70.5. Interestingly, a discernible trend emerged, indicating a decrease in K:Rb ratios moving northeastward. Sample MO-019 displayed the lowest K:Rb ratio at 59, the only ratio falling below 60 among the ten samples. The two samples with the lowest ratios, MO-019 and MO-014, were retrieved from claims 50 and 243, respectively. Samples MO-012, -014, -015, and -020 exhibited K:Rb ratios ranging between 60 and 70, while samples MO-013 and -016 showcased ratios within the 70-80 range. Remarkably, sample MO-003 recorded the highest K:Rb ratio at 85.

MO-003	MO-011	MO-012	MO-013	MO-014	MO-015	MO-016	MO-017	MO-019	MO-020
85.4	95.1	67.2	71.0	62.2	62.9	77.2	62.5	59.1	62.5

Table 4: Potassium / rubidium ratios of pegmatite samples.

Discussion

The company pegmatite exploration project has a fairly standard lithium-cesum-tantalum (LCT) geologic setting (Bradley et al., 2017). It may be compared to other historically productive LCT pegmatites. The pegmatite is hosted in a metamorphic terrain, enveloped in quartz-mica schist, similar to other pegmatites such as the Black Hills LCT pegmatites in South Dakota. It is also magmatically derived from granites like the Black Hills and Pala, southern California, LCT pegmatites (Jahns and Wright, 1951; Norton and Others, 1964).

The geometry of the company's pegmatite is much akin to the local Arizona LCT pegmatites described previously by Jahns (1952). The tabular sheetlike morphology of the tilted dikes is also similar to that of the Sitting Bull pegmatite in the Black Hills (Figure 12), and the major Greenbushes pegmatite of West Australia (Norton et al., 1964; Ingham et al., 2012). The 200 ft thickness of the pegmatite is consistent with technical observations of nearby pegmatites by the neighboring exploration company (Bradda Head Lithium Ltd., 2023). The field observations of the northeasterly linear trend at a 45º dip within the study area appears to continue further into the company claim block (Figures 4, 5).

The minerals in the samples are consistent with LCT pegmatites and demonstrate that the pegmatites is geochemically not homogenous. Surface samples have the right mineralogy of quartz, albite, and muscovite with accessory schorl (Figure 9) as nearby previously productive lithium pegmatites, as described by Jahns (1952) and London and Burt (1978). Average mineralogy matches that of spodumene – bearing lithium pegmatite ore fields in central China, like those in Figure 14 (Bai et al., 2023). The change to blocky K-feldspar in proximity to the historical P&G Beryl mine suggests the exposure of an inner layer of the pegmatite to surface (Figure 11).

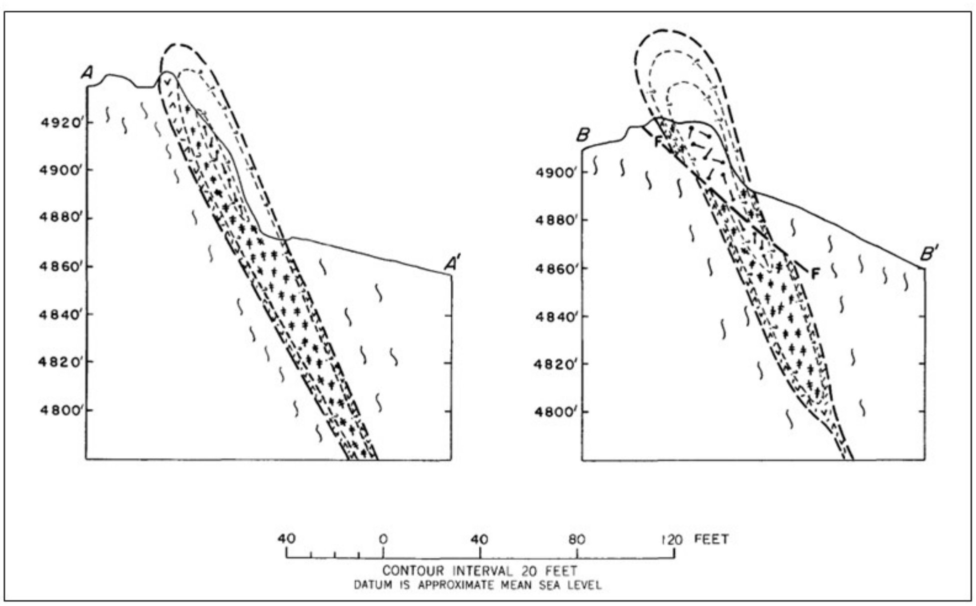

Figure 13: Sitting Bull pegmatite cross section, SD, USA.
Note the tabular geometry and tilted orientation of the pegmatite dike. From Norton and Others (1964).

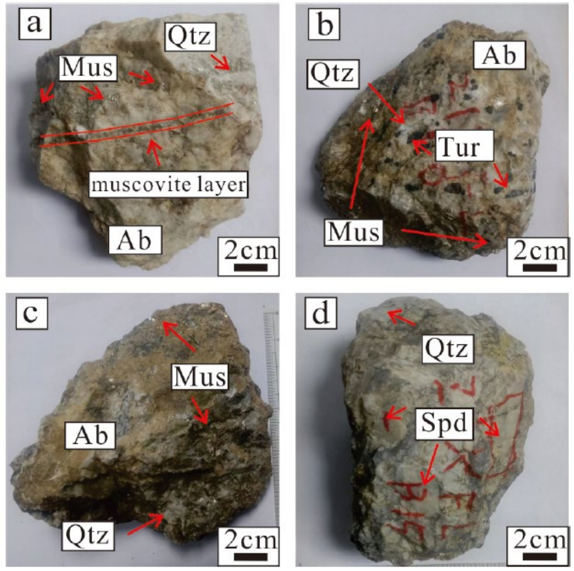

Figure 14: Samples from a foreign, spodumene bearing pegmatite.
Those samples are of pegmatite zones, external to internal, from a-d respectively. Spodumene is innermost zone. Qtz = quartz, Mus = muscovite, Ab = albite, Tur = tourmaline, Spd = spodumene. From Bai et al., 2023.

The assay results in Table 3 are common in early exploration stage campaigns (Rose et al., 1979). The nature of lithium mineralization within the volume of the pegmatite dyke may occur in lenses and pods distributed throughout Jahns (1952). Empirical evidence from soil sampling campaigns has found that pegmatites are compositionally heterogeneous along strike, such as that in Figure 15 (Patriot Lithium, 2023). This is encouraging that higher lithium values will be discovered nearby. Additionally, pegmatites are zoned, and there is a strong likelihood that the lithium will be within the pegmatite.

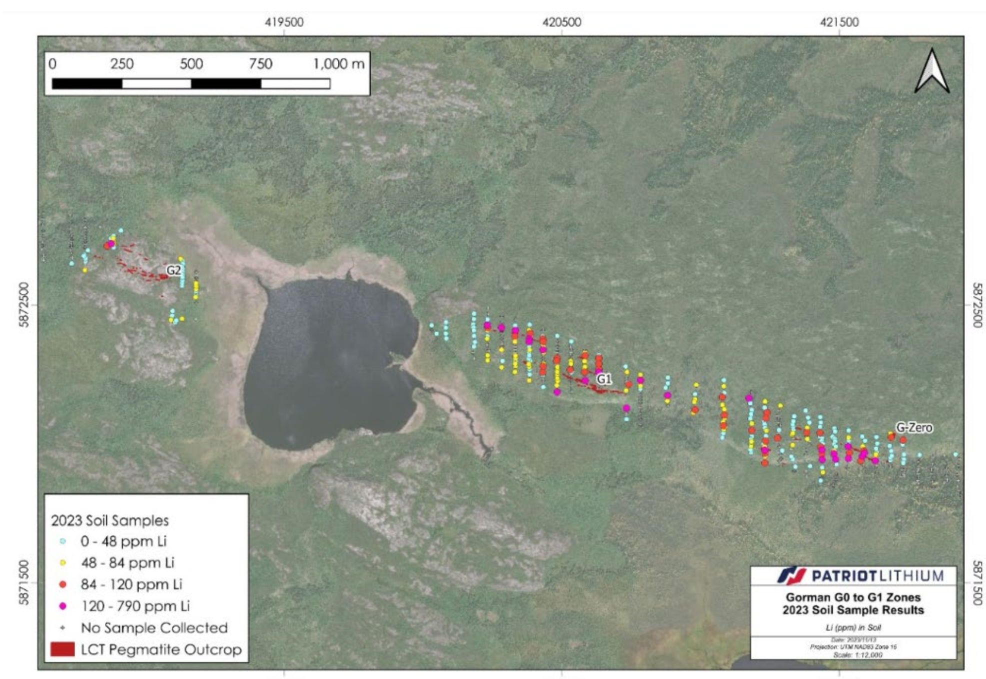

Figure 15, previous: Example Canadian pegmatite soil sampling assays.
The contrast of lithium concentrations highlights the pegmatite. From Patriot Lithium (2023).

The use of K:Rb ratios remains a standard geochemical vectoring method in searching for LCT pegmatites (Černý, 1991; Steiner, 2019). Comparison of M.O. project K:Rb ratios with maximums for spodumene-bearing pegmatites ratios places the project within the boundaries for spodumene pegmatite discovery (Figure 16). The lowering of the K:Rb ratio from southwest to northeast across the property is indicative of more highly fractionated rock in that direction. It is possible that the ratios continue to lower and thereby increase lithium mineralization potential towards the northeast.

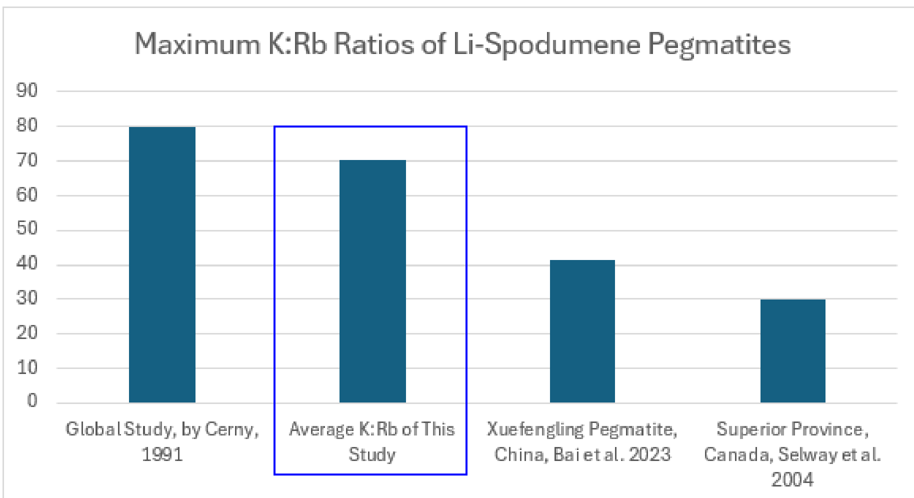

Figure 16: Comparison of maximum LCT K:Rb ratios to BRGC project average.
Data from this study, Černý (1991), Selway et al. (2004), and Bai et al. (2023).

Future Work

The Midnight Owl Pegmatite Exploration Project has shown strong potential to bearing lithium minerals towards the northeast on the exposed pegmatite strike. The mineralogy and geology of the pegmatite is like those previously examined in the USA, Canada, and China. Mapping results have shown the direction and geometry the pegmatite.

These results combine to lead the company to the next steps:

1. Soil sampling survey at the regional scale. Lines with 200 m sample spacing from east to west across the property.

2. Soil sampling at the local scale. Polygons with 25m sample spacing where evidence of pegmatite has been found.

The sample lines and polygon will be akin to those in Figure 17. Sediments will be tested for lithium and associated pathfinder elements such as potassium, rubidium, cesium, tantalum, beryllium, and others. This level of investigation will be sufficient to illuminate if there is lithium mineralization potential in the area.

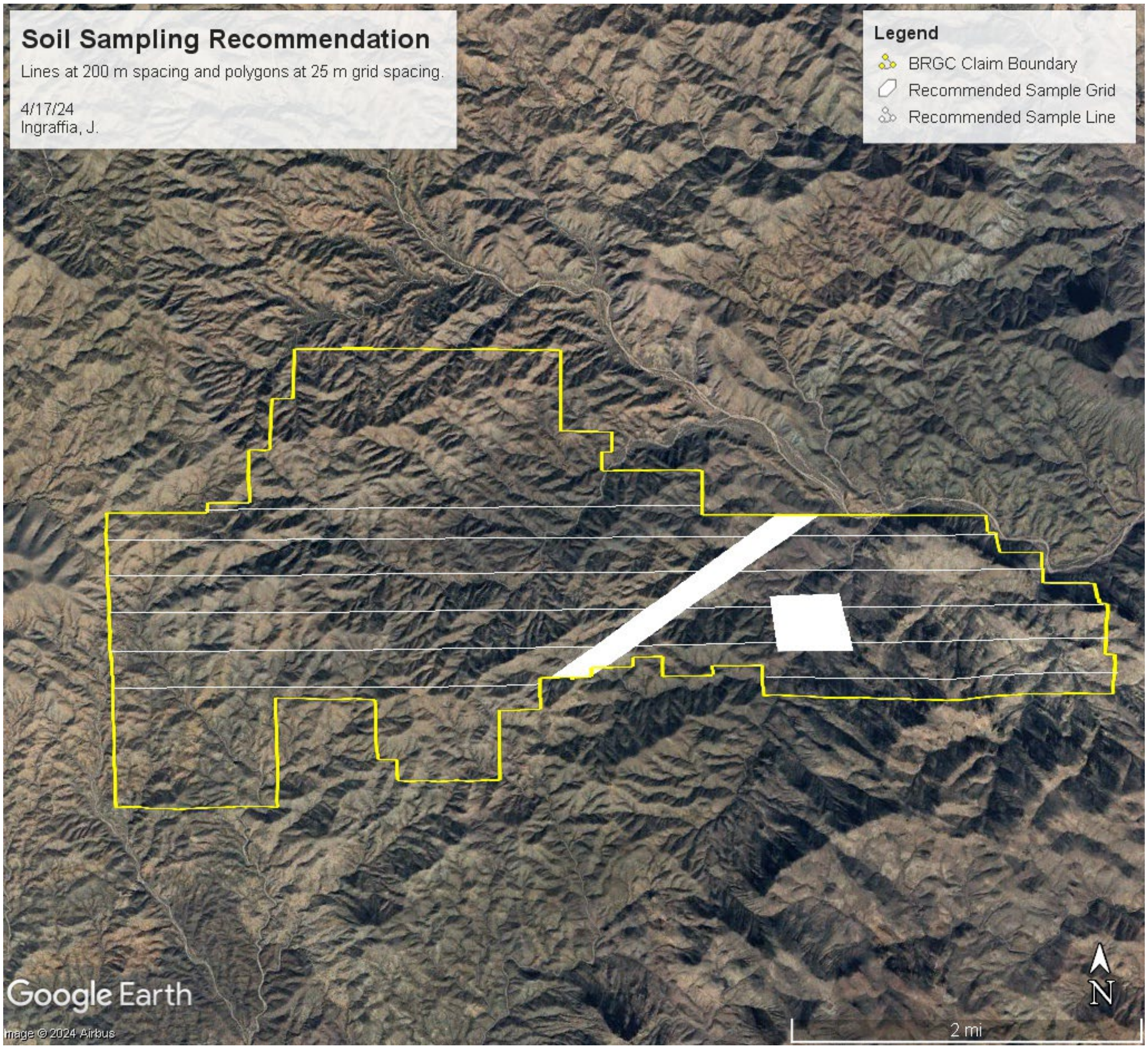

Figure 17: Soil sampling lines and polygons in the BRGC Li Pegmatite claim block.
The lines will take samples at 200 m spacing. The polygons will have a 25 m sample spacing grid.

References

Ascarza, W. (2017, Sept. 10). Mine Tales: Arizona Mines Supply Beryllium, Important to Defense Industries. *Arizona Daily Star*.

Bai, H.Y., Wang, H., Zhang, X.Y., Zhu, B.Z., Wang, K.Y., Huang, L. (2023). The origin of Xuefengling rare metal pegmatites and implications for ore. *Ore Geology Reviews, Volume 163*.

Bradda Head Lithium Ltd. (2023). *San Domingo Overview*. Retrieved from Bradda Head Lithium Ltd., Accessed Mar. 10, 2023: https://www.braddaheadltd.com/projects/san-domingo

Bradley, D., McCauley, A., and Stillings, L. (2017). *Mineral-Deposit Model for Lithium-Cesium-Tantalum Pegmatites.* Reston, Virgina: U.S. Geological Survey, Chapter 0 of Mineral Deposit Models for Resource Assessment, Scientific Investigations Report 2010-5070-0.

Brightrock Gold Corp. (2023, August 22). *BrightRock Gold Corporation Announces the First-of-its-Kind Discovery of a Significant Spodumene Deposit at its Midnight Owl Location near Wickenburg, Arizona Using SpecTir Hyperspectral Data*. Retrieved from Accesswire: https://www.accesswire.com/775905/brightrock-gold-corporation-announces-the-first-of-its-kind-discovery-of-a-significant-spodumene-deposit-at-its-midnight-owl-location-near-wickenburg-arizona-using-spectir-hyperspectral-data

Brightrock Gold Corp. (2022, July 18). *A look at the last XRF readings taken from our Midnight Owl Mine in 2017 by the previous owners.* Retrieved from Twitter: https://twitter.com/brightrock_corp/status/1549040032308072452?s=46

Černý, P. (1991). Rare-element Granitic Pegmatites. Part I: Anatomy and. *Geoscience Canada, 18(2)*, 49-67.

Guilbert, J.M., and Park, C.F. (1986). *The Geology of Ore Deposits.* Long Grove, IL: Waveland Press.

Ingham, P. D., White, I. R., and Jackson, S. (2012). *Greenbushes Lithium Operations.* Sydney, Australia: 43-101 Technical Report prepared for Talison Lithium Limited by Behre Dolbear Australia Pty Limited.

Jahns, R. (1952). Pegmatite Deposits of the White Picacho District. *University of Arizona Bulletin, Arizona Bureau of Mines, Vol. 23*.

Jahns, R.H., and Wright, L.A. (1951). Gem- and Lithium-Bearing Pegmatites of the Pala District, San Diego County, California. *Special Report 7-A, U.S. Division of Mines*.

London, D., and Burt, D. (1978). *Lithium Pegmatites of the White Picacho District, Maricopa and Yavapai Counties [with road log], Arizona.* in Burt, D.M., and Pewe, T.L., eds., Guidebook to the geology of central Arizona, 74th Cordilleran Section Meeting, Geological Society of America, Arizona State University, Tempe, Arizona: Arizona Bureau of Geology and Mineral Technology Special Paper no.

London, D., and Burt, D.M. (1982). Alteration of spodumene, montebrasite and lithophilite in pegmatites of the White Picacho District, Arizona. *American Mineralogist, Volume 67*, 97-113.

Meeves, H.C., and Others. (1966). Reconnaissance of Beryllium-Bearing Pegmatite Deposits in Six. *IC Bureau of Mines Information Circular 8298. U.S. Dept of the Interior, Bureau of Mines*.

Mindat. (2024). *Mindat*. Retrieved from Mindat.org, Accessed Mar. 10, 2024: https://www.mindat.org/loc-41247.html

Norton, J.J. and Others. (1964). *Geology and Mineral Deposits of Some Pegmatites in the Southern Black Hills, South Dakota.* Washington D.C.: U.S. Geological Survery, Professional Paper 297-E, U.S. Government Printing Office.
Patriot Lithium. (2023). *Gorman Soil Sampling Identifies 1.5 km Continuous Lithium Anomaly.* ASX Announcement.
Rose, A.W., Hawkes, H.E., and Webb, J.S. (1979). *Geochemistry in Mineral Exploration, Second Ed.* New York: Academic Press.
Selway, J.B., Breaks, F.W., and Tindle, A.G. (2005). A Review of Rare-Element (Li-Cs-Ta) Pegmatite Exploration Techniques for the Superior Province, Canada, and Large Worldwide Tantalum Deposits. *Exploration and Mining Geology, Vol. 14, Nos. 1-4*, 1-30.
Steiner, B. (2019). Tools and Workflows for Grassroots Li–Cs–Ta (LCT). *Minerals*.
Sunderland, A. (2023). Pers. Comm.